JOURNAL OF MATERIALS SCIENCE 33 (1998) 3233–3244

The structure and properties of spray formed cold rolling mill work roll steels

D. N. HANLON, W. M. RAINFORTH, C. M. SELLARS
The University of Sheffield, Department of Engineering Materials, Sheffield, UK
E-mail: m.rainforth@sheffield.ac.uk

R. PRICE, H. T. GISBORNE
Forged Rolls UK Ltd, Sheffield, UK

J. FORREST
Osprey Metals Ltd, Neath, UK

A study of the effect of spray casting on the microstructure and properties of cold rolling mill work roll steels has been undertaken. Industry standard qualities have been spray formed and a comparison of the resulting properties and microstructures has been made with those of the conventionally processed counterparts. The influence of process variables on the spray formed product has also been investigated. The results indicate that cold mill work roll steels which have comparable properties and structures to conventionally cast and forged products can be produced successfully in a single processing step. Furthermore, a high integrity metallurgical bond between the deposit and the substrate can be achieved.

1. Introduction

Cold rolling mill work rolls must operate under extremely arduous conditions. They are subjected to high cyclic stresses and extensive abrasion. These mechanisms each contribute to deterioration of the surface quality of the mill work roll and thus drastically affect the quality and dimensional tolerance of the rolled product. All rolling mills must establish a schedule for regular roll maintenance in order to produce products of consistent quality. Mill down time, from planned roll changes, and unscheduled stoppages, is responsible for a considerable loss of revenue in the rolling industries. Extending the working life of rolling mill work rolls therefore has considerable commercial appeal.

The property requirements of rolling mill work rolls are many and varied. In general, the working surface must posses high strength, a high resistance to wear, high fatigue resistance and be sufficiently tough to withstand impacts and overloads. These property requirements are often contradictory, for instance a high resistance to wear is normally associated with high hardness [1] and therefore correspondingly low fracture toughness. As with many products an acceptable balance of properties must be sought. This is achieved by tailoring the composition and manipulating the microstructure.

Microstructures which contain high volume fractions of hard, alloy carbide phases are known to be highly wear resistant [2]. However, cold mills rolls are currently manufactured by ingot casting and forging and these conventional processing routes impose severe restrictions on the alloy compositions from which rolls may be made. Highly alloyed steels undergo pronounced macro-segregation during ingot solidification and consequently have highly inhomogeneous microstructures comprising coarse, interconected eutectic carbides. Such interconnected carbides are highly detrimental to toughness and fatigue resistance [2]. Therefore, if highly alloyed materials are to be exploited, control of the homogeneity and scale of the microstructure is paramount.

The spray forming process has found numerous applications since its conception by Singer [3]. It allows the production of near net shaped components which are free of macro-segregation and display a high degree of microstructural refinement in a single processing step [4]. It has been successfully applied to the production of a variety of product forms including billets, tubes and strips [4]. The process which has been described in detail in numerous other texts [4] essentially entails atomizing liquid metal using a high pressure gas (usually nitrogen in the case of steels) and collecting the atomized droplets onto a moving substrate. Ideally the droplets are semi-solid at the moment of deposition and repeated impact of particles maintains a mushy zone at the surface in which the dendritic solidification structure is repeatedly destroyed. The nucleation frequency in this zone is high and this yields a dense, segregation-free microstructure which is, in comparison with conventionally cast alloys, greatly refined in scale. Thus, spray casting is particularly well suited to the production of highly alloyed grades

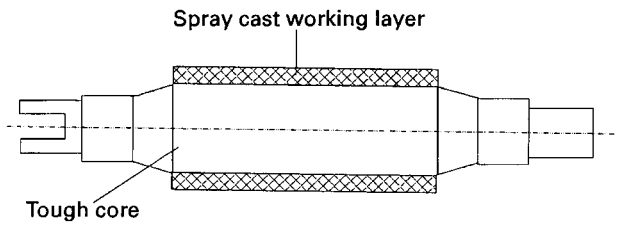

Figure 1 Diagram illustrating the duplex spray formed roll.

which undergo pronounced segregation and for which microstructural refinement by mechanical working is prohibited.

A further advantage of spray forming is that it enables the production of a composite product. In the case of mill work rolls careful materials selection provides the potential to produce a duplex roll (Fig. 1) with a tough, damage-tolerant core (substrate material) with an overlay of a hard wear resistant material (deposit) as the working surface. However, for this to be successful, a high quality metallurgical bond must be achieved between the deposit and the substrate. The development of bonded products using the Osprey process is still in its infancy [5].

This paper presents the key findings of a study which has been undertaken to determine the effect of spray forming on the microstructure and properties of currently adopted cold mill work roll steels (carbon-chromium steels) and to assess the viability of the process for work roll manufacture. Detailed microstructural characterization is reported along with details of the response to heat treatment, tensile properties and wear resistance. Direct comparison has been made with conventionally produced material. The effects of processing parameters on the quality of the deposit/substrate bond are discussed.

2. Experimental procedure

Two industry standard cold rolling mill work roll steels, a 0.8C/3Cr steel and a 0.8C/5Cr steel, have been investigated. The full analyses of each of these materials, as established using the inductively coupled plasma (ICP) technique, are listed in Table I. Experimental samples of each alloy were produced by both conventional and spray forming processing techniques.

The conventionally processed material was produced by the ingot casting and forging route in a manner similar to that currently used for rolling mill work roll manufacture. However, in order that laboratory scale samples could be produced, the bulk of the conventionally processed material was subjected to a far heavier forging reduction than is normal during the manufacture of mill rolls. A small number of samples were also sectioned from full section mill rolls to provide a direct comparison with the more lightly forged materials found in service. These conditions are hereafter referred to as heavily forged and lightly forged conditions, respectively.

Spray forming was used to produce small scale billets of round cross-section, of nominally 100 mm diameter, under a range of deposition conditions. The liquid steel was atomized by a high pressure gas (nitrogen) and the resulting spray of liquid droplets was deposited onto a rotating tubular mild steel collector. The deposition temperature of the droplets was controlled by the gas/liquid metal ratio during the atomization process. Various gas/metal ratios were investigated to give a range of deposition conditions from 'hot' to 'cold'. The ranges of deposition conditions used for each material are listed in Table II where they are expressed as a gas/metal ratio.

All materials were subjected to hardening and tempering heat treatments (austenitization for 1 h at 880 °C, oil quenching and tempering at between 200 and 500 °C for one hour). Mechanical properties were evaluated using Vickers hardness and tensile testing techniques. Tensile testing was conducted on the 0.8C/5Cr steel in both the spray cast and heavily forged conditions. All specimens were tested in the hardened condition (tempered to a comparable hardness of 750–800 H_v). Elevated temperature tensile tests were also conducted at 500 °C using hardened specimens.

All wear testing was conducted using a Cameron Plint multi-purpose friction and wear testing machine in a rolling/sliding testing configuration (described in greater detail elsewhere [6]) as illustrated schematically in Fig. 2. A rolling sliding wear testing configuration was used since this technique most closely imitates the conditions found in service for cold rolling mill work rolls. In this configuration wear may result from the high alternating stresses experienced during rolling contact (rolling contact fatigue based mechanisms-RCF) or from the relative motion between

TABLE I Chemical analysis of conventionally processed (heavily forged) and spray cast 0.8/3Cr and 0.8C/5Cr alloys

		C	Cr	Mn	Ni	Mo	S	P	Si	Cu
5Cr	Standard	0.78	4.71	0.25	0.21	0.21	0.001	0.013	0.58	0.16
	Spray cast cold	0.77	5.28	0.24	0.19	0.19	0.002	0.006	0.63	0.12
	Spray cast medium	0.77	5.23	0.24	0.19	0.19	0.002	0.006	0.59	0.12
	Spray cast hot	0.75	5.08	0.24	0.19	0.20	0.002	0.006	0.58	0.12
3Cr	Standard	0.81	3.10	0.29	0.30	0.24	0.001	0.014	0.31	0.14
	Spray cast cold	0.77	3.20	0.23	0.22	0.18	0.002	0.11	0.17	0.12
	Spray cast medium	0.78	3.28	0.24	0.26	0.20	0.002	0.011	0.19	0.12
	Spray cast hot	0.76	3.26	0.23	0.22	0.18	0.002	0.011	0.21	0.12

TABLE II Casting conditions used for production of the small scale spray cast billets

Material	Spray conditions	Gas/metal ratio ($m^3\ kg^{-1}$)
5Cr	Cold	0.66
	Medium	0.59
	Hot	0.52
3Cr	Cold	0.67
	Medium	0.63
	Hot	0.59

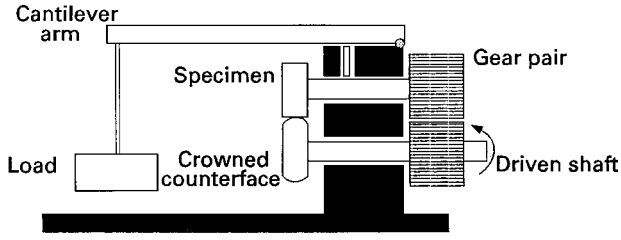

Figure 2 Schematic illustration of the rolling sliding contact wear test configuration.

counterface and specimen (sliding wear based mechanisms). Wear test specimens were produced with a range of hardness values by hardening and tempering for 1 h at various temperatures between 200 °C and 500 °C. Specimens were ground to final dimensions after heat treatment (to a 1200 grit finish) in order to remove decarburized and oxidized layers. An applied load of 300 N and a rotation speed of 500 r.p.m. (approximately $1.6\ m\ s^{-1}$) with a slippage of 8% between the specimen and the counterface were employed. All tests were run for a total distance of approximately 70 km (i.e. a distance which yielded an appreciable wear volume). Wear was evaluated by measurement of weight loss ($\pm$ 1 mg). In all cases the counterface material used was M2 tool steel hardened and tempered to a hardness of approximately 850–900 H_v.

The microstructure of all materials, wear surfaces, wear profiles and tensile fracture surfaces were studied using optical microscopy, scanning electron microscopy (SEM) (Jeol 6400), transmission electron microscopy (TEM) (Jeol 200 CX and Philips 420) and energy dispersive X-ray spectroscopy (EDS) (Oxford Instruments). Iron and alloy-carbide identification and size determination was conducted in the TEM using a single stage carbon-extraction replication technique. The diameters of individual carbide particles were measured directly from bright field TEM micrographs. A minimum of 300 particles were measured for each condition studied. Quantification of EDS traces was undertaken using predetermined Cliff–Lorimer factors. Only thin areas of the sample were used so that the thin sample approximation was applicable and absorption effects could be ignored. The volume fraction of carbides present in spray cast and conventionally cast materials was evaluated by means of electrolytic extraction using a 10% HCl solution as the electrolyte.

Trials to evaluate deposit/substrate bond formation during spray casting were conducted on a larger scale. Full details of the roll production assembly and the large scale production unit development have been published elsewhere [5]. For the bond trials reported here a 30–35 mm 0.8C/5Cr deposit was laid onto a 170 mm diameter forged steel arbor (also 0.8C/5Cr). Substrate pre-heating was achieved by means of an induction heating assembly [5]. The substrate was first bulk pre-heated by passing the substrate through the induction coil a number of times. The required surface temperature was then achieved by flash pre-heating as the coil was translated along the arbor just in advance of the spraying nozzle. The full thickness of the deposit was laid in a single pass [5] onto arbors pre-heated to a range of temperatures. The substrate temperature just in advance of the spray was measured throughout the process by means of optical pyrometry. However, due to the confined space and the consequent build up of recirculating powder in the spray chamber the results obtained are considered unreliable. Because of the difficulties associated with temperature evaluation, and also, in part, the proprietry nature of the pre-heat temperature data, all pre-heat values are reported in terms of the induction coil power output (Table III). The bond strength was evaluated using tensile testing. Tensile specimens were sectioned across the interface such that the interface lay at the centre of the gauge and the tensile axis of the specimen was normal to the interface (Fig. 3). Specimens were tested in the hardened condition (austenitization at 880 °C followed by an oil quench and tempering at 350 °C). Tensile tests were also conducted using specimens sectioned from the bulk of the deposit remote from the interface and which had been subjected to the same heat treatment.

TABLE III Mean power input during flash pre-heating cycle for large scale bond evaluation trials (power input is proportional to flash temperature rise)

Trial	Flash pre-heat temperature (mean induction coil power input, (kW))
A	295
B	340
C	360
D	400

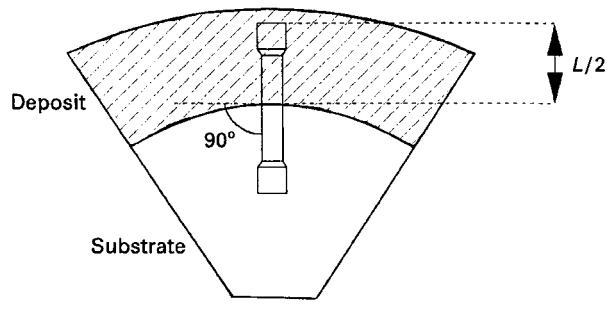

Figure 3 Diagram illustrating the location from which cross bond tensile test pieces were sectioned.

3. Results

3.1. Microstructures

All spray cast billets produced were of high integrity containing only a limited amount of porosity present as a few isolated pores in the bulk of the deposit. The volume fraction of these pores was too low to quantify using point counting techniques.

For the spray formed conditions the as-received microstructure was found to consist essentially of pearlite with a lamellar distribution of carbides in a ferritic matrix (Fig. 4). The microstructure of the forged materials on the other hand consisted of spheroidal carbides in a ferritic matrix prior to receipt. Sparse networks of coarser proeutecoid carbides were observed on prior austenite grain boundaries, particularly in the case of the 0.8C/5Cr composition.

The microstructures of all steels in the quenched and tempered condition consisted of martensite containing a uniform distribution of resolvable carbides. The carbides were now discrete and spheroidal in all materials as illustrated in Fig. 5.

The hardening responses of the spray-cast and forged materials are illustrated in the temper curves shown in Fig. 6. This figure indicates that the as-quenched hardness is higher for the spray-cast materials than for their forged counterparts for both the 0.8C/3Cr and 0.8C/5Cr materials. Spraying conditions were not found to have a significant affect on the heat treatment response of these materials.

The results of quantitative EDS (Table IV) indicate that the principal carbide type present in each of the two steels is different. The average Fe/Cr ratio was 2.7

Figure 4 Secondary electron SEM micrograph showing lammellar carbides as observed in all spray cast materials in the as-sprayed condition.

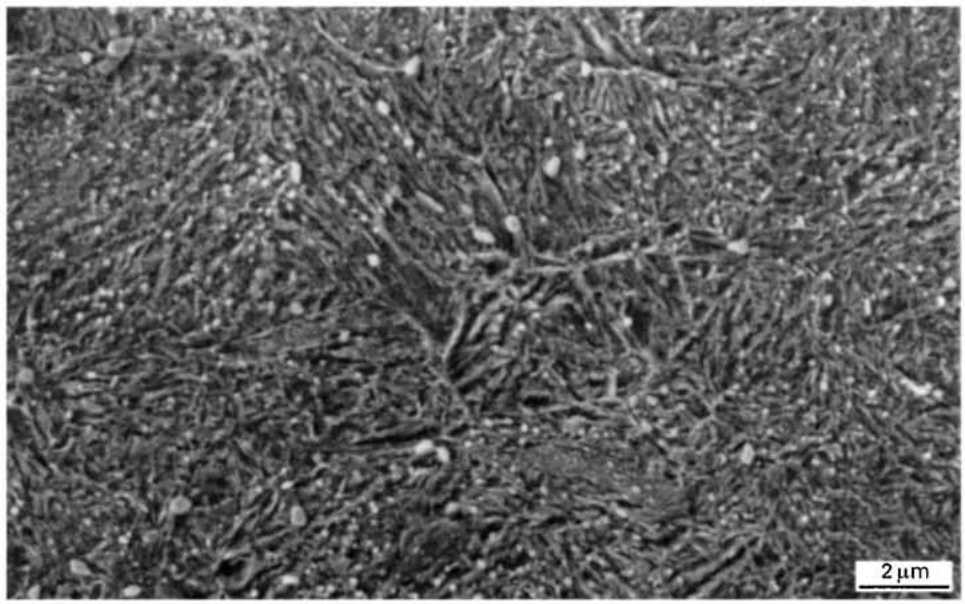

Figure 5 Secondary electron SEM micrograph showing the typical microstructure as observed in all spray cast materials in the hardened condition.

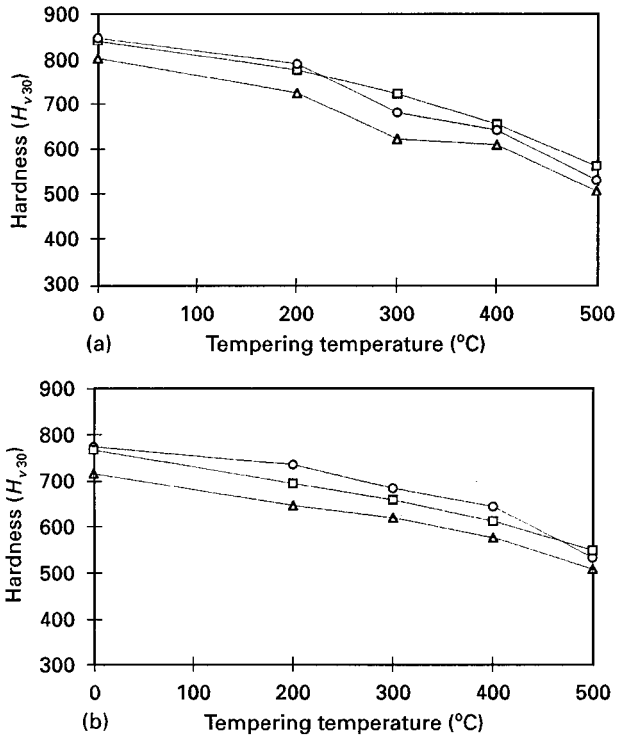

Figure 6 Variation of Vickers hardness (Hv_{30}) with tempering temperature for: (a) 0.8C/3Cr and (b) 0.8C/5Cr (□ spray cast (cold), ○ spray cast (hot), △ heavily forged).

for the carbides observed in the 0.8C/3Cr alloy and 0.97 (with the exception of a small (<5%) number of carbides which contained higher Cr levels) for the 0.8C/5Cr alloy. These results are broadly consistent with those reported in the literature for Fe_3C (Fe/Cr $\approx$ 1) and $(FeCr)_7C_3$(Fe/Cr $\approx$ 3) which are the expected equilibrium phases in the 0.8C/3Cr and 0.8C/5Cr steels, respectively.

Selected area diffraction (SAD) in the TEM, the results of which are summarized in Fig. 7, confirmed the EDS observations. The iron rich phase observed in the 0.8C/3Cr composition was found to be orthorhombic and hence Fe_3C (Fig. 7a) whilst the chromium rich phase was identified as having a hexagonal structure and hence is $(Cr,Fe)_7C_3$ (Fig. 7b). Streaking was also observed in SAD patterns obtained from the chromium rich phase (Fig. 7c), associated with faulting of the carbide and is a feature which is typical of $(Cr,Fe)_7C_3$. Thus the predominant carbide phase is each alloy composition was different, with that in the 0.8C/5Cr almost exclusively the more chromium rich $(Cr,Fe)_7C_3$ carbide with occasional Fe_3C carbides while the 0.8C/3Cr material contained only $(Fe,Cr)_3C$. Spray forming did not change the carbide type present in the hardened condition for either the 0.8C/3Cr or the 0.8C/5Cr compositions. Electrolytic extraction experiments conducted on the 0.8C/5Cr materials indicated that spray forming had no measurable influence on the volume fraction of carbide in the quenched and tempered condition, as demonstrated by the results for the 0.8C/5Cr composition given in Table V.

The most significant effect of spray forming on the microstructure was its influence on the average carbide size and carbide size distribution. The results of carbide size measurements are summarized in Table VI. The carbide size distributions observed for the variously processed 0.8C/5Cr materials are also shown in the histogram in Fig. 8. The mean size of the carbides found in the spray cast materials is smaller than that found in either the heavily forged or the lightly forged material. The carbide size distribution was narrower for the spray cast material, and was skewed for the conventionally processed materials which contained a greater number of coarse carbides. The maximum carbide size present was strongly influenced by the processing route. Spray cast material exhibited a maximum carbide size of approximately 0.5 μm while the conventionally processed materials exhibited maximum carbide sizes of 1.0 μm for the heavily forged and 2.0 μm for the lightly forged material. Variations in the gas/metal ratio were not found to influence the carbide size in the spray cast materials.

3.2. Tensile testing

The results of tensile testing are summarized in Table VII. These results indicate that spray cast material exhibits a significantly lower tensile strength

TABLE IV Quantitative analysis of carbide particles observed in extraction replicas taken from the 0.8C/3Cr and 0.8C/5Cr qualities

Material	Reading	Quantity of iron		Quantity of chromium		Fe/Cr ratio
		wt %	at %	wt %	at %	
0.8C/5Cr	Particle 1	47.33	45.18	51.57	52.86	0.87
	Particle 2	52.97	50.96	46.46	48.01	1.06
	Particle 3	47.38	45.20	51.41	52.56	0.86
	Particle 4	47.94	45.90	51.28	52.74	0.87
	Particle 5	57.45	55.62	42.36	44.05	1.26
	Average	50.61	48.57	48.62	50.07	0.97
0.8C/3Cr	Particle 1	74.07	72.68	25.93	27.32	2.66
	Particle 2	74.04	72.64	25.96	27.36	2.65
	Particle 3	74.45	73.07	25.55	26.93	2.71
	Particle 4	75.25	73.90	24.75	26.10	2.83
	Particle 5	74.27	74.30	25.73	25.70	2.89
	Particle 6	74.18	72.79	25.82	27.21	2.68
	Particle 7	74.32	74.93	25.68	27.07	2.77
	Average	74.36	73.47	25.63	26.81	2.74

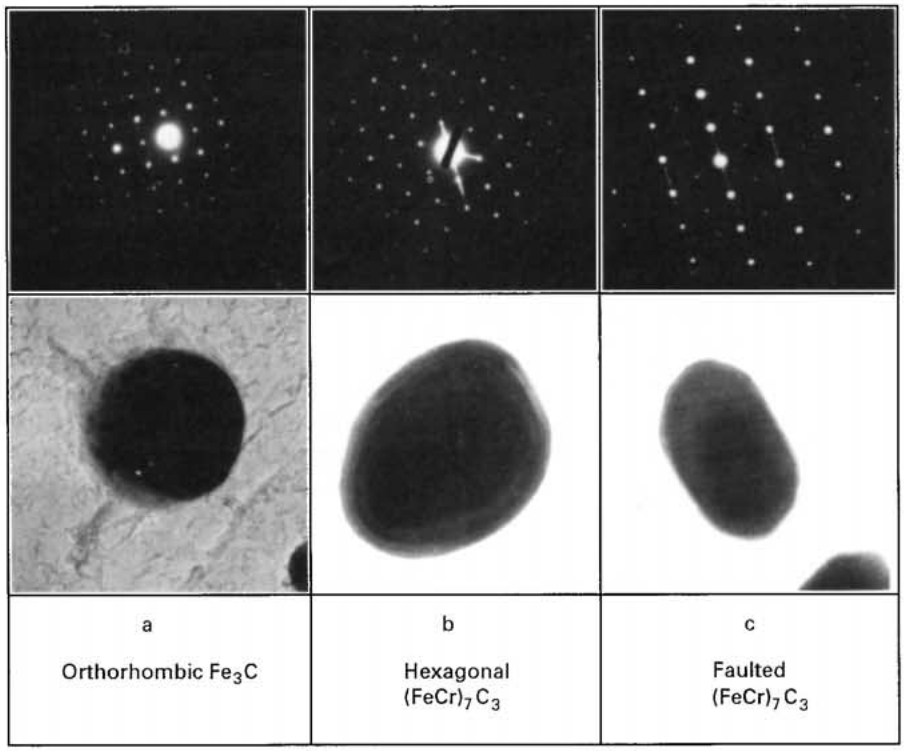

Figure 7 Carbide identification as determined using SAD in TEM, carbide in (a) is ≈ 400 nm wide, in (b) ≈ 200 nm wide and in (c) the longest dimension is 240 nm.

TABLE V The fraction of carbides by weight in heavily forged and spray cast 0.8C/5Cr as determined using a chemical extraction technique

Material	Fraction of carbide by weight (%)
Spray cast 0.8C/5Cr	4.1(± 0.41)
Heavily forged 0.8C/5Cr	3.7(± 0.37)

TABLE VI Mean and maximum carbide sizes for all 0.8C/3Cr and 0.8C/5Cr conditions studied

Specimen	Mean carbide size (μm)	Maximum carbide size (μm)
Spray cast 0.8C/3Cr	0.13	0.6
Heavily forged 0.8C/3Cr	0.20	1.1
Lightly forged roll 0.8C/3Cr	0.45	1.6
Spray cast 0.8C/5Cr	0.13	0.5
Heavily forged 0.8C/5Cr	0.21	0.9
Lightly forged roll 0.8C/5Cr	0.44	2.0

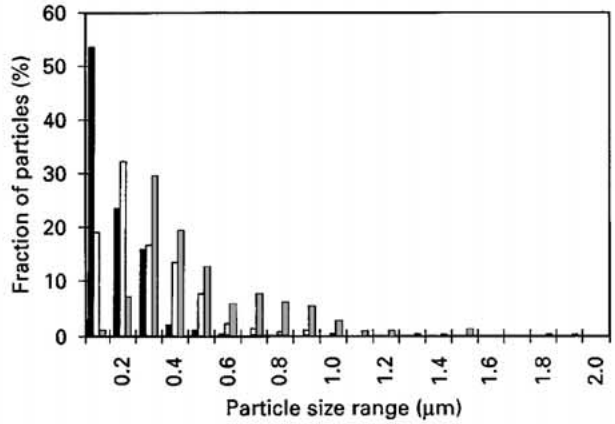

Figure 8 Histogram showing the particle size distributions observed in spray cast, (■) heavily forged (□) and lightly forged (▩) 0.8C/5Cr materials.

than heavily forged material when tested at ambient temperature in the hardened condition. However, when the same materials were tested at elevated temperature, the tensile strengths of each were identical. In the case of the hardened material tested at ambient temperature, the ductility of both the spray cast and forged material was close to zero. For the elevated temperature tests on the hardened material the tensile ductility of the spray cast material was lower than that of the forged material.

When tested at ambient temperature in the hardened condition the failure modes of both conventionally processed and spray cast material were similar. The fracture halves in both cases were flat and normal to the tensile axis. The fracture surfaces were both characterized by ductile dimples (Fig. 9) indicating a ductile failure mode (microvoid nucleation and coalescence) even though the macro behaviour was brittle. Occasional regions of porosity were observed on the surface of the spray cast specimens (Fig. 10).

At elevated temperatures both the spray cast and the heavily forged material underwent ductile fracture.

TABLE VII Results of tensile tests conducted at ambient and elevated temperature (**curve did not exhibit sufficient offset to report 0.1% PS)

Condition	Specimen	Test temp. (°C)	0.1% proof stress ($N mm^{-2}$)	Ultimate tensile strength ($N mm^{-2}$)	Reduction in area (%)	Actual specimen hardness (H_v)
Forged	5Cr	20	1859	1967	0	752
Sprayed	5Cr (014 Cold)	20	–	**1036	0	792
Sprayed	5Cr (015 Medium)	20	–	**991	0	786
Sprayed	5Cr (017 Hot)	20	–	**1097	0	790
Forged	5Cr	500	1240	1255	33.0	–
Sprayed	5Cr (014 Cold)	500	1216	1230	10.7	–
Sprayed	5Cr (014 Medium)	500	1252	1267	3.2	–
Sprayed	5Cr (017 Hot)	500	1222	1236	3.5	–

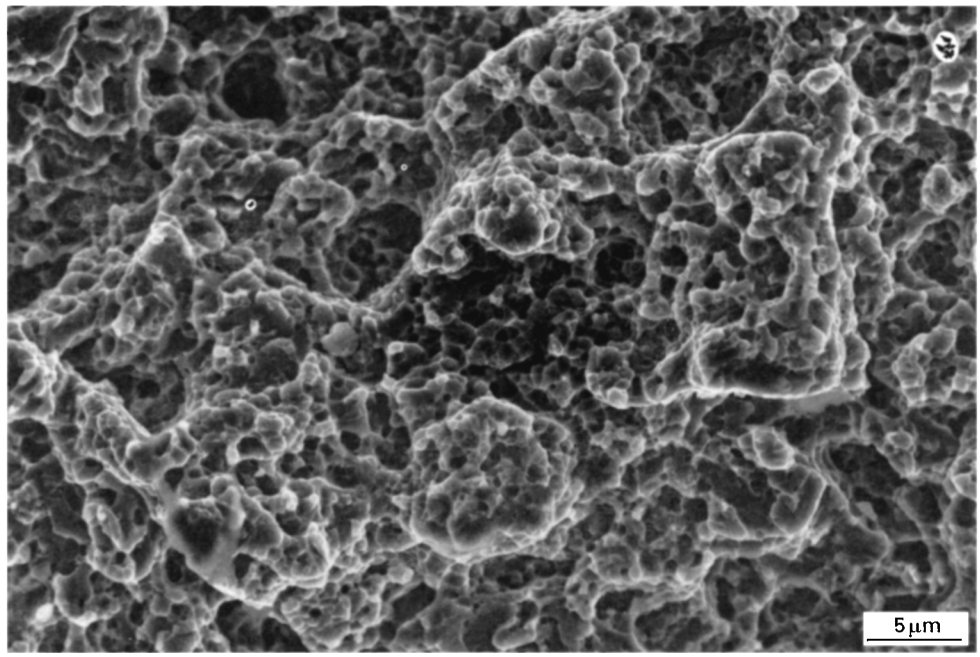

Figure 9 Secondary electron SEM fractograph showing ductile dimples as observed on the fracture surface of a hardened 0.8C/5Cr tensile test piece tested at ambient temperature.

In the case of the spray cast material initiation was found to have occurred at porosity (Fig. 10).

3.3. Wear testing

The variation in wear response with initial specimen hardness (temper condition) is shown in Fig. 11. Wear rate is expressed as a dimensional coefficient k (after Lanchester [7]) where:-

$$k = \frac{V}{LD}$$

Here; V = volume loss, L = applied load and D = sliding distance. Larger values of k denote higher rates of wear.

These results indicate that the principal microstructural factor effecting wear is matrix hardness. All of the variously processed materials (spray formed, heavily forged and lightly forged 0.8C/3Cr and 0.8C/5Cr steels) yield wear data which are indiscrenible from one another.

3.4. Bond trials

Low magnification micrographs of the interface region of the lowest and highest pre-heat casts (295 kW and 400 kW mean power inputs, respectively) are shown in Fig. 12. In the case of the 295 kW pre-heat the bond was found to be discontinuous. In addition, a broad (4 mm), dense band of coarse base porosity was observed close to the interface. For the 400 kW specimen a low volume of basal porosity was observed, in a 1.5 mm broad band, close to the interface in some locations. No evidence of debonding could be found and, when viewed at higher magnifications, the interface appeared diffuse and no distinct border between the deposit and substrate structures could be found (Fig. 13).

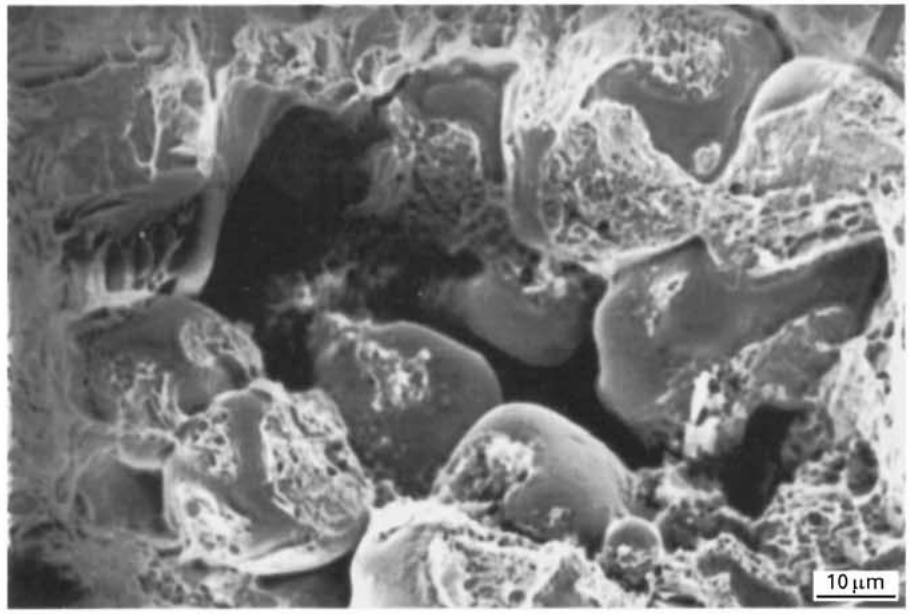

Figure 10 Secondary electron SEM fractograph showing micro-porosity and prior atomised particles as observed on the fracture surface of a hardened, spray cast 0.8C/5Cr tensile test piece tested at ambient temperature.

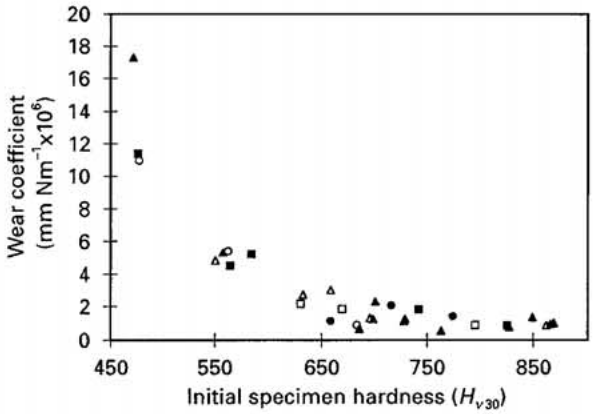

Figure 11 Variation of wear coefficient with initial specimen hardness for all 0.8C/3Cr and 0.8C/5Cr rolling sliding contact tests. △ 3Cr Spray cast 300N, □ 3Cr Heavily forged, ○ 3Cr Lightly forged roll 300N, ▲ 5Cr Spray cast 300N, ■ 5Cr Heavily forged 300N, ● 5Cr Lightly forged roll 300N.

The results of the cross bond tensile tests are summarized graphically in Fig. 14. The average fracture stress recorded across the bond was found to increase with increasing substrate pre-heat temperature. The maximum cross bond UTS observed for the 295 kW roll was approximately 30% of the deposit UTS whilst that observed for the 400 kW flash pre-heat was approximately 86% of the deposit UTS.

Observation of the fracture surfaces of failed specimen halves revealed that cross bond tensile specimens exhibited three failure modes. Specimens sectioned from bond trials conducted at the 295 kW and 340 kW preheats failed exclusively at the interface. Failure remote from the interface was observed for specimens sectioned from the bond trial conducted at the 400 kW pre-heat. Specimens taken from the trial conducted at the intermediate preheat of 360 kW were found to have failed in the porous basal region close to the interface or by a mixture of interfacial and base porosity modes. These observations are illustrated in the low magnification SEM fractographs in Fig. 15.

At higher magnifications the substrate half fracture surfaces of interfacially failed specimens are comprised of flat, featureless regions with discrete spray droplets attached and small islands of ductile microvoids (Fig. 16a). On the deposit half, the fracture surface comprises of porous regions in which prior atomized particles are visible (Fig. 16b) and areas which have undergone microvoid coalescence. Thus, it would appear that restricted regions have been successfully bonded to the substrate. In the case of failure which occurred in the deposit remote from the interface the failure mode was seen to be identical to that observed for the bulk tensile test pieces. Porosity was again observed on the fracture surfaces. No direct evidence (river lines, etc.) could be found which pinpointed the location of fracture initiation but pores are the most likely sites of fracture initiation.

4. Discussion

4.1. Microstructure and properties

The results indicate that high integrity pre-forms may be produced from existing cold mill roll steel grades using the Osprey process. On the basis of carbide size evaluation experiments the microstructure of spray formed samples was found to be marginally finer than that of a heavily forged condition. In both alloys, whether spray cast or conventionally processed, the carbide phases present were those expected at equilibrium [8]. Furthermore, spray forming caused no pronounced depletion of the major alloying elements.

Variations in the casting parameters imposed did not measurably affect the scale of the microstructure of the small scale spray cast billets. This contradicts much previously published work which has shown

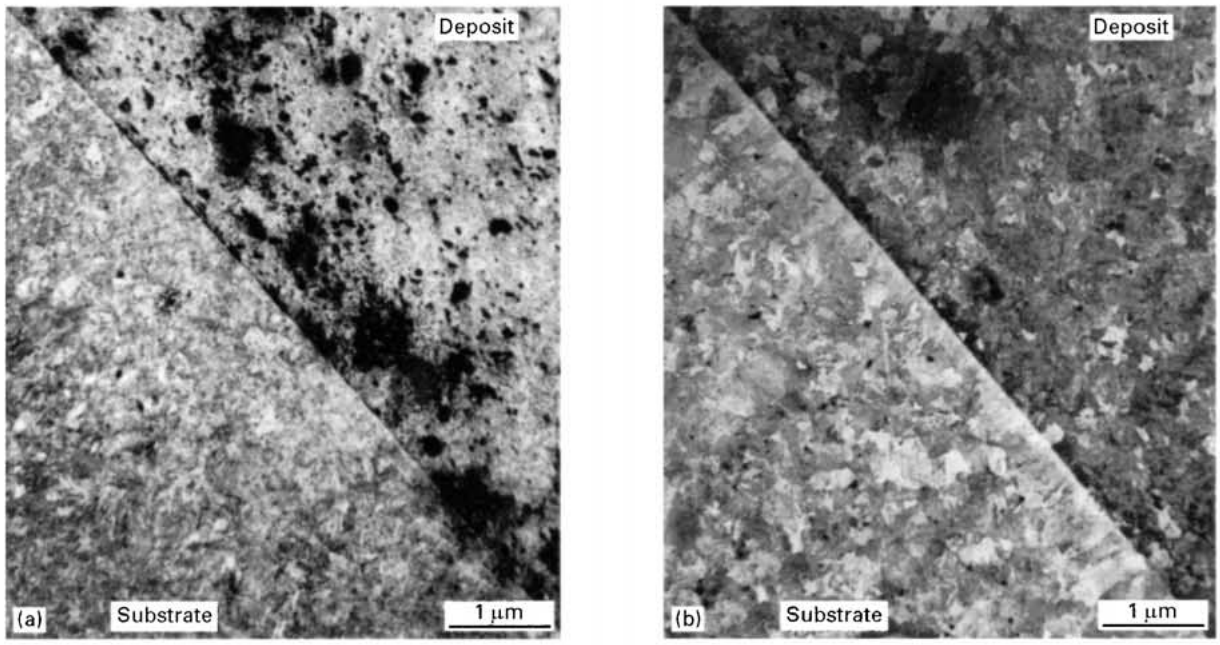

Figure 12 Low magnification optical micrographs showing the microstructure at the interface of large scale bond evaluation trial sprays conducted at the highest and lowest power input trials (corresponding to the lowest and highest flash pre-heat temperatures). (a) 295 kW mean power input, (b) 400 kW mean power input.

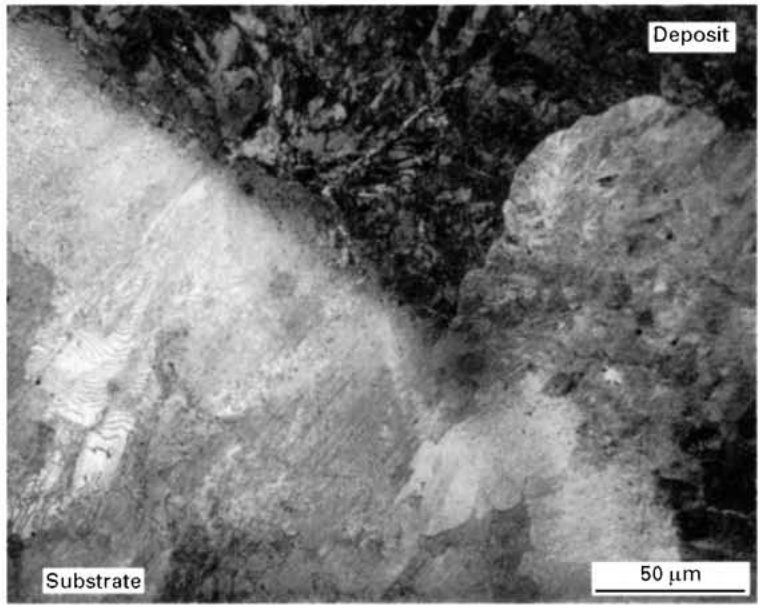

Figure 13 High magnification optical micrographs showing the interface region of a high integrity metallurgical bond as achieved using a 1300 °C flash pre-heat temperature.

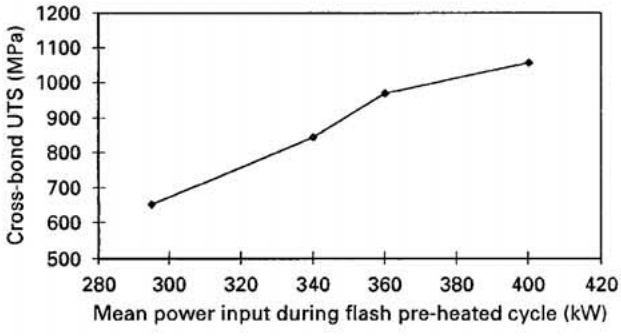

Figure 14 Variation of average cross bond fracture stress with mean power input during flash pre-heat cycle of large scale bond trails (0.8C/5Cr deposit on 0.8C/5C substrate).

that for ferrous alloys variations in the gas to metal volume ratio (G/M) have a pronounced influence on the scale of the resulting microstructure [9]. However, much of this work has concentrated on more highly alloyed materials where the carbide forms directly from the liquid phase. In such materials the G/M ratio is found to influence the size and distribution of primary phases or eutectics which form from the liquid. In the case of the steels investigated here, the equilibrium structure is largely formed via the eutectoid reaction [8]. During spray casting, the initial cooling of the atomized droplets by convection during flight is rapid. However, after deposition the cooling rate through the solidus to room temperature is

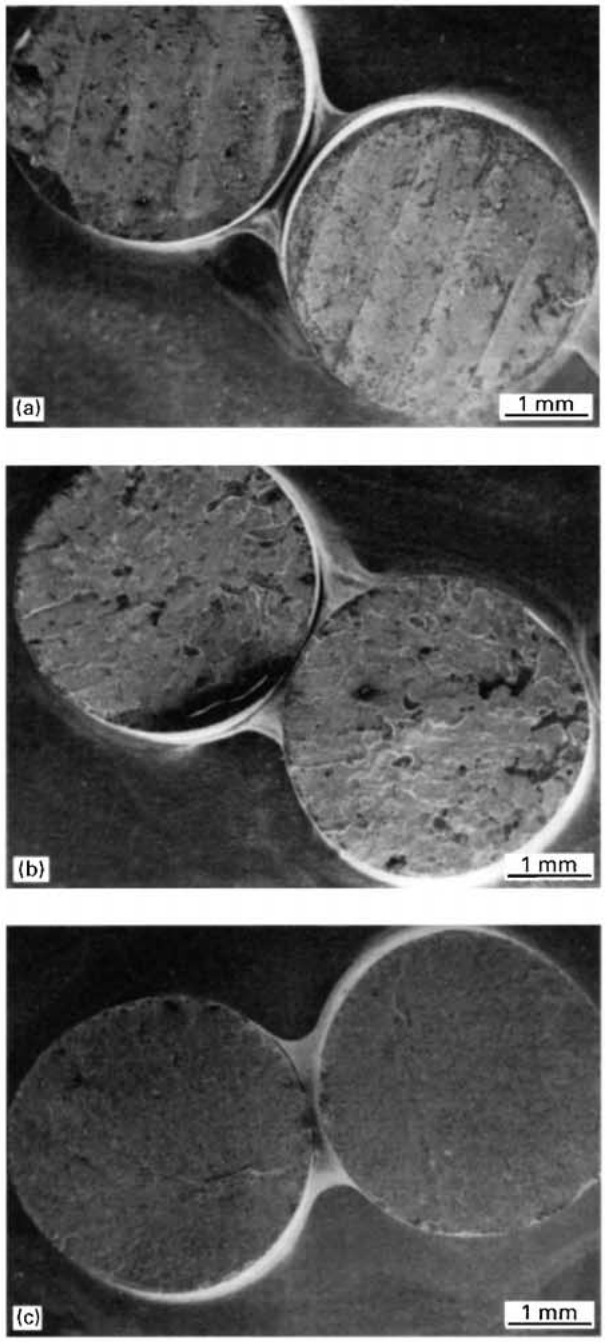

Figure 15 Low magnification secondary electron SEM fractographs showing three modes of failure observed for cross bond tensile specimens (a) interfacial failure, (b) interfacial/basal porosity failure, (c) deposit failure.

comparable to that achieved during conventional processing. Therefore, the influence of casting parameters can only have an indirect effect on the final structure produced through solid state transformations via their effect on prior austenite grain size.

The response to heat treatment for the spray cast material was found to differ from that of the conventional material. The as-quenched hardness was consistently higher for the spray cast materials than for the conventional materials. There are several possible explanations for this difference; namely, a greater retention of carbon in solid solution as a result of the processing (leading to enhanced solid solution strengthening) and/or a finer prior austenite grain size (leading to a smaller martensite packet size and consequently a greater Hall–Petch strengthening contribution). Given the finer carbide size found in the spray cast material it seems probable that carbide resolution during heat treatment would occur more rapidly and that the former explanation is thus more likely.

The wear response of both the conventionally processed and spray cast materials was used as the principal basis for comparison of properties. The wear response of all materials tested, whether 0.8C/3Cr or 0.8C/5Cr, was comparable. The principal factor effecting wear response was found to be the matrix hardness (temper condition). The variation in carbide size observed for the various materials had no measurable effect on wear. It also appears that the presence of porosity in the spray cast material did not detrimentally effect the wear behaviour. Observations of wear surfaces and wear surface cross-sections indicated that a complex combination of wear mechanisms was in operation including rolling contact fatigue (RCF), abrasion and oxidation. The extent of oxide coverage observed on the worn surfaces suggests that an oxidational wear mechanism was dominant. This would explain the absence of an effect of carbide size since oxidative wear is not sensitive to such microstructural variables. The full details of the wear behaviour are reported elsewhere [6].

4.2. Interface adherence

The results of the larger scale bond evaluation work indicate that for the steels investigated, a high integrity metallurgical bond can be achieved via the single pass deposition technique. Cross bond tensile strengths in excess of 1200 MPa have been recorded for trials conducted using the highest substrate pre-heat achieved using a mean power input of 400 kW. This UTS is some 85% of that recorded for tensile test pieces taken from the bulk of the deposit. Substrate pre-heat temperature influences the cross bond tensile behaviour through both its effect on the continuity of the metallurgical bond and its effect on the volume of basal porosity in the deposit close to the interface. Increasing the pre-heat temperature has been shown to both improve bond integrity (reducing the extent of debonding at the interface) and reduce the extent (both in terms of density and band width) of basal porosity.

Whalroos and Liimitainen [10] showed that for a stainless steel deposited onto a mild steel tube a threshold pre-heat temperature (in the range 600–1000 °C) existed below which a bond was not achieved. These authors concluded that increasing the temperature beyond this threshold yielded no further improvement in the adherence of the deposit even though this led to a reduction in the extent of interfacial porosity. These authors reported only the results of tests which for which failure occurred at the interface. The average interfacial (tensile) bond strength after deposition at a substrate pre-heat of 1000 °C was approximately 500 MPa.

During the work reported here the deposit was found to adhere to the substrate for all pre-heat

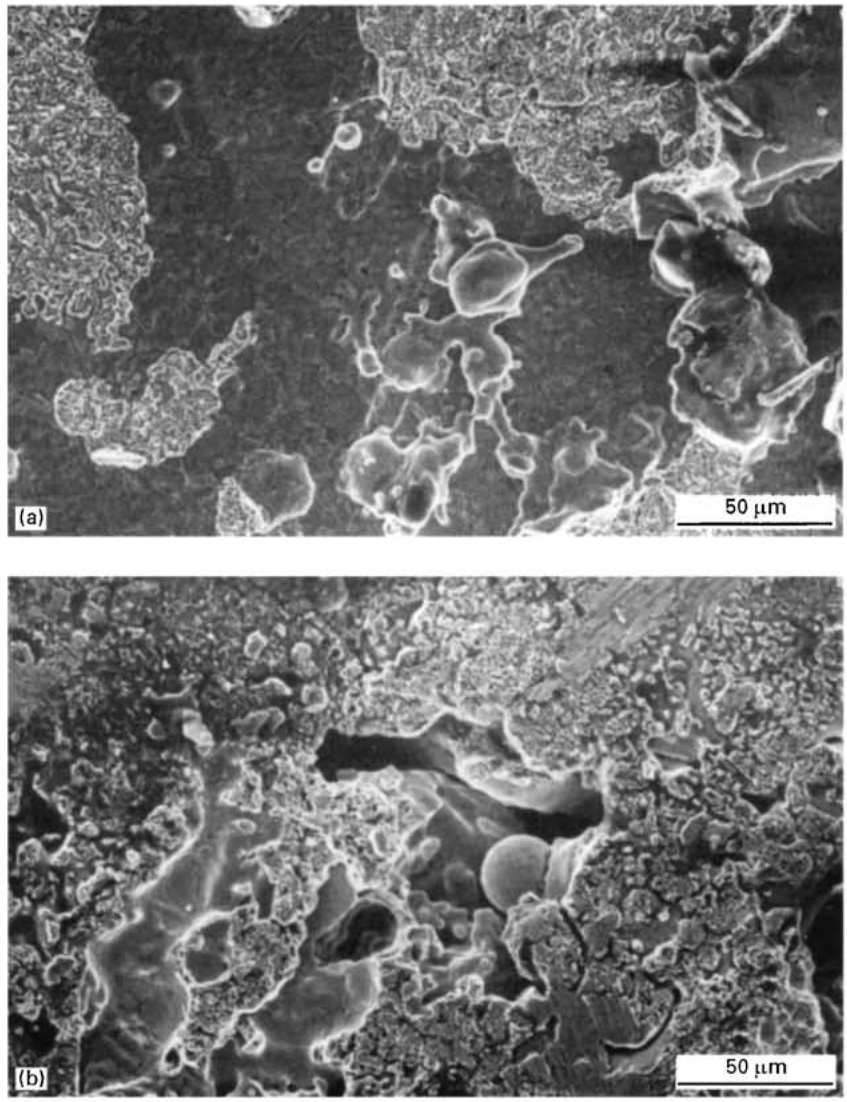

Figure 16 High magnification secondary electron SEM fractographs showing (a) interfacial failure and (b) failure in basal porosity.

temperatures thus suggesting that the threshold temperature for bonding as defined by Wharloos and Liimitainen [10] was exceeded at the lowest pre-heat temperature (at a mean power input of 295 kW). Here, the results of tests which failed both at and remote from the interface are reported and the values recorded represent either the strength of the bond or of the weakest microstructural link. At this lowest pre-heat an average cross bond tensile strength of approximately 640 MPa was recorded.

In contrast to the work of Wahlroos and Liimitainen [10] further increasing the level of pre-heat beyond the bonding threshold was found to improve cross bond tensile strength with the maximum bond strength occurring for the highest pre-heat temperature (achieved using a mean power input of 400 kW). For these conditions an average strength of 1050 MPa was recorded across the bond. Since failure occurred remote from the bond in this case, the value represents the strength of the deposit and that of the bond must be higher.

The results of tensile testing conducted on the small scale casts (Table VII) indicated that UTS in these high hardness, brittle materials is directly affected by the presence of porosity. As the ductility of the material was increased (testing at elevated temperature) the influence of porosity was seen to diminish. Thus, it would seem that for the bond trials (which were conducted on hardened material at ambient temperature) the cross bond tensile properties are dependent on the extent of basal porosity formation. The work of Wahlroos and Liimitainen [10] was conducted on materials with a greater ductility than those considered here and hence the defect tolerance of these materials may have been higher.

5. Conclusions

1. The Osprey process can be used to produce high integrity performs of cold rolling mill work roll steels with microstructures comparable to those of heavily forged conditions.

2. High densities were achieved in spray formed materials. However, even the low volume fraction ($< 1\%$) of porosity detrimentally affected tenile properties in high hardness tempers.

3. Spray forming produced a high as quenched hardness in the conventionally processed material. This higher hardness was retained on tempering for 1 h at temperatures of up to 500 °C for both 0.8C/3Cr and 0.8C/5Cr materials.

4. Spray forming did not alter the carbide type present. However, a finer carbide size was found in spray formed material (0.13 μm) compared to heavily forged (0.2 μm) and lightly forged, commercial material (0.45 μm).

5. The rolling/sliding wear response of spray formed materials is indistinguishable from that of conventionally processed material.

6. A high integrity metallurgical bond can be achieved using the single pass deposition technique by means of substrate pre-heating.

7. Increasing the substrate pre-heat temperature increases the cross bond UTS through its effect on bond quality and on the density of basal porosity formed.

Acknowlegements

This work was funded by the EPSRC-DTI-Link scheme for Enhanced Engineering Materials. Thanks go to Dr. I. R. Reaney and Mr R. I. Kangley for assistance with practical aspects of the work.

References

1. J. F. ARCHARD and W. HIRST, *Proc. Roy. Soc.* A **236** (1956) 397–410.
2. C. P. TABRETT, I. R. SARE and M. R. GHOMASHCHI, *Int. Mater. Rev.* **41** (1996) 59.
3. A. R. E. SINGER, *Metall. Mater.* **4** (1970) 246.
4. A. G. LEATHAM, R. G. BROOKS and M. YAMAN, "Modern Developments in Powder Metallurgy", Vols 15–17 (Metal Powder Industries Federation, Princeton, NJ, USA, 1985).
5. J. FORREST, R. PRICE and D. HANLON, *Int. J. Powder Metall.* **33** (1997) 21.
6. D. N. HANLON, W. M. RAINFORTH and C. M. SELLARS, *Wear* **203–204** (1997) 220.
7. J. K. LANCASTER, *ibid.* **10** (1967) 103.
8. V. G. RIVLIN, *Int. Met. Rev.* **29** (1984) 299.
9. Y. IKAWA, T. ITAMI, K. KUMAGAI, Y. KAMASHIMA, A. G. LEATHAM, J. S. COOMBS and R. G. BROOKS, *ISIJ Int.* **30** (1990) 756.
10. J. M. WHALROOS and T. P. LIIMATAINEN, Proceedings of ICSF Conference **2** (1993) 225.

Received 2 February
and accepted 7 April 1998